Investigation on the ion velocity distribution in the magnetic nozzle of an ECR plasma thruster using LIF measurements

IEPC-2017-382

Julien Jarrige[1], Sara Correyero[2], Paul-Quentin Elias[3], Denis Packan[4]
ONERA-The French Aerospace Lab, Palaiseau, France

Abstract: Laser-induced fluorescence (LIF) is a non-intrusive technique that can provide useful information on ion production and acceleration in electric propulsion system. In this paper, spatially resolved LIF measurements of Xe^+ are performed in the plume of an electron cyclotron resonance plasma thruster. The mapping of ion velocity distribution function in the magnetic nozzle shows that the ions are accelerated over a distance greater than 12 cm. A mean axial velocity up to 16 km/s has been obtained at 1 sccm and 26 W. The acceleration of ions is compared for different xenon flowrates.

Nomenclature

ECR	=	electron cyclotron resonance
FP	=	Fabry-Perot
IVDF	=	ion velocity distribution function
LIF	=	laser induced fluorescence
LP	=	Langmuir probe
V_z	=	mean axial velocity (at the position z)
V_∞	=	asymptotic axial velocity
z	=	longitudinal position in the magnetic nozzle
λ_0	=	transition wavelength
ν_L	=	laser frequency
φ	=	electrostatic potential (at the position z)
φ_0	=	plasma potential in the ECR source
φ_∞	=	asymptotic potential

I.   Introduction

IN the last few years, electrodeless plasma thrusters that make use of a magnetic nozzle (like the helicon thruster or the ECR plasma thruster) have received a great attention for their ability to accelerate simultaneously electrons and ions. These electrodeless thrusters are current-free, so that no electron-emitting neutralizer is required, which could significantly reduce the development costs and failure risks in operation.

---

[1] Research Scientist, Physics Instrumentation and Space Department, julien.jarrige@onera.fr.
[2] PhD student, Physics Instrumentation and Space Department, sara.correyero@onera.fr.
[3] Research Scientist, Physics Instrumentation and Space Department, paul-quentin.elias@onera.fr.
[4] Research Scientist, Physics Instrumentation and Space Department, denis.packan@onera.fr.

The electron cyclotron resonance (ECR) plasma thruster that is currently being developed by ONERA has shown very promising performances in the thrust range 0.1-1 mN. A thruster efficiency as high as 16% has been deduced from electrostatic probes measurement, with an ion energy up to 300 eV [1, 2]. The performances have been confirmed recently by direct thrust measurements on a thrust balance [3].

The study of physical mechanisms in magnetic nozzle is still an active field of research. Several theoretical and numerical studies have been led to understand the underlying mechanisms, e.g. electron detachment, electron cooling, and ion acceleration [4, 5, 6, 7]. Although the models have shown how the ambipolar electric field is formed in the plume, there is no complete self-consistent model that can simulate the ion acceleration. Moreover some hypotheses must be made on electron dynamics. Therefore there is a real need for experimental data on plasma properties in the plume of magnetic nozzle thrusters.

Laser-induced fluorescence (LIF) is a non-intrusive measurement technique that has been shown to provide a wealth of information on plasma species, including ions. It has been successfully applied on several thrusters technologies like HET or FEEP [8, 9, 10]. LIF is particularly useful to measure the ion velocity distribution function (IVDF). Recently, a 3D tomographic reconstruction of the full IVDF in the phase of space has been performed in the plume a HET [11 ,12].

In this paper, we present a study of the acceleration of xenon ions in the magnetic nozzle of the ECR plasma thruster using LIF technique. The IVDF of Xe^+ is measured at different positions along the axis of the magnetic nozzle. The mean axial velocity and the plasma potential profiles are compared for different xenon mass flowrates.

II.   Methods and apparatus

A. ECR plasma thruster

All LIF measurements presented in this paper are performed on the ECR plasma thruster model with a permanent magnet (ECR-PM). This ECR-PM thruster consists of a semi-open coaxial cavity 27.5 mm in diameter and 15 mm in length (see schematic in Figure 1). The magnetic field that is necessary for the resonance effect and the magnetic nozzle acceleration is provided by an annular permanent magnet with an axial magnetic moment. The magnetic field configuration of the thruster is a magnetic mirror: the magnetic field is purely divergent in the source and the nozzle. As can be seen in Figure 2, the resonant region for a microwave excitation of 2.45 GHz (*i.e.* B = 875 Gauss) is located 2 mm away from the back of the source.

The back of the source is covered with a non-conductive plate made of boron nitride. The outer cylinder and the inner conductor are made of carbon graphite and stainless steel, respectively.

The thruster is operated with microwave power at a frequency of 2.45 GHz. The power absorbed by the plasma is measured using a directional coupler that is located on the RF coaxial feedthrough of the vacuum chamber. Forward and reflected powers are measured with calibrated diodes. The attenuation of microwave power through the cables and connectors on the vacuum side is about 0.55 dB.

The thruster is fed with xenon through small injection holes in the backplate using a Brooks 5850E mass flow controller. A picture of the ECR thruster operated with xenon (2 sccm) is shown in Figure 1.
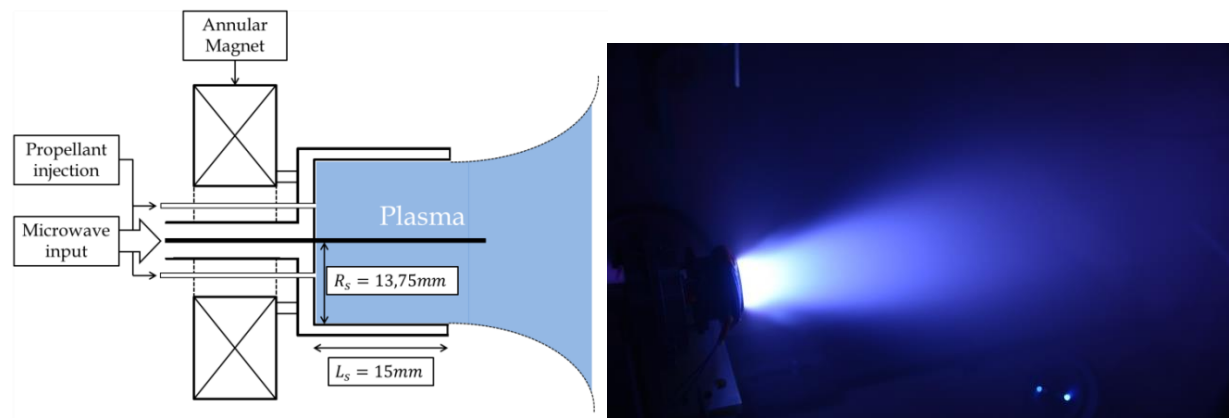

Figure 1.   Schematic of the permanent magnet ECR plasma thruster and image of the thruster operated with xenon.
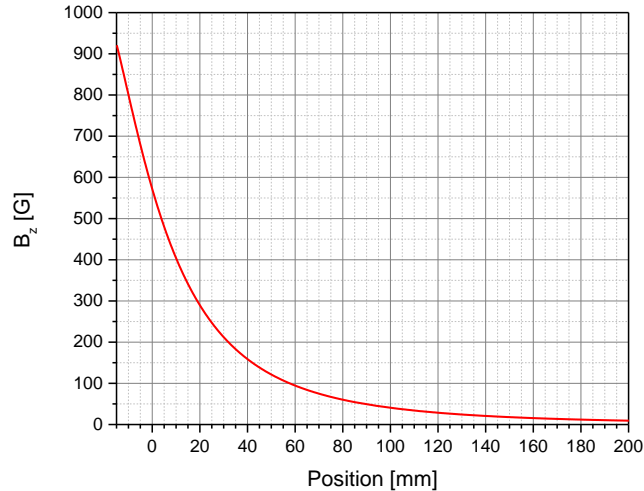
Figure 2. Longitudinal profile of the magnetic field. Position z=-15 mm refers to the backplate of the thruster, and z=0 to the thruster exit.

B. LIF scheme and IVDF

Laser induced fluorescence measurements are performed by probing the $5d[4]_{7/2}$ - $6p[3]_{5/2}$ electronic transition of Xe^+ at 834.724 nm (834.955 nm in vacuum). This scheme starts from a metastable state (not the ground state). The laser pumps the ion metastable to a higher energy state, and the fluorescence signal, which results from a radiative decay to a third state, is collected at 541.915 nm. This multilevel scheme enables to reject the parasitic light from the laser.

The measurement of ion velocity distribution is based on the Doppler effect. Assuming that the transition frequency is v_0 (for ions at rest), a population of ions with a velocity V along the laser axis (counter-propagating) will be pumped at a slightly different laser frequency v_L such as:

$$V = \lambda_0(v_0 - v_L)$$

Under appropriate conditions, the intensity of the fluorescence signal is proportional to the number of ions with a velocity V in the measurement volume. The ion velocity distribution function can then be obtained by measuring the fluorescence signal when sweeping the laser wavelength.

C. Laser optical setup and LIF acquisition system

A schematic diagram of the optical setup is shown in Figure 3. The laser source is a SDL-TC10 external cavity tunable diode laser centered at 834.7 nm. Fine tuning of the laser wavelength can be obtained by adjusting the position of the grating with a piezo-driver actuator. The output power is about 20 mW, with a mode-hop free tuning range up to 60 GHz and a linewidth of 200 kHz. In this work, typical measurements are performed with a frequency span of 25 GHz, which allows the measurement of ions with a velocity up to 21 km/s (*i.e.* ion energy up to 300 eV).

The laser wavelength is monitored with a LM007 4-Fizeau interferometers wavemeter. During LIF measurements, the laser frequency is swept by applying a ramp of voltage to the piezo-electric actuator. The laser frequency is determined accurately using a Fabry-Perot (FP) etalon and a reference discharge. This method is detailed in section D.

The laser beam is chopped using an acousto-optic modulator with a 50% duty cycle. The laser is sent alternatively in the reference arm and in the thruster measurement arm.

The fluorescence light from the thruster and the reference discharge is collected in optical fibers and fed to Hamamatsu photomultipliers tubes (PMT). Interference filters centered at 540 nm with a 10 nm bandpass enable to partly reject parasitic light from the plasma. The fluorescence signal is then amplified using lock-in amplifiers (EG&G 5210 for the reference signal, SR830 for the thruster signal).

The acquisition of the PMT (thruster and reference) and photodiode (FP) signals, and the control of the piezo-driver voltage for the laser frequency scan are performed with a National Instruments PCI 6251 DAQ board.

3

The measurement parameters used in this work are listed in Table 1. Inside the source and in the near-field region of the plume, LIF signal is high enough to perform short acquisitions (<1 min). In the far field region (typically z>65 mm), a longer lock-in time constant is required to efficiently filter the fluorescence signal from the ambient noise. The sweep time then needs to be adjusted in order to keep constant the frequency resolution of the measurement.

Assuming that the lock-in amplifier cannot separate peaks closer than 3 times the time constant, it comes that the frequency resolution of the measurement is about 1.2 GHz. So ion population peaks with a velocity difference higher than 1 km/s can be distinguished on fluorescence spectra.

Table 1.   LIF measurements parameters

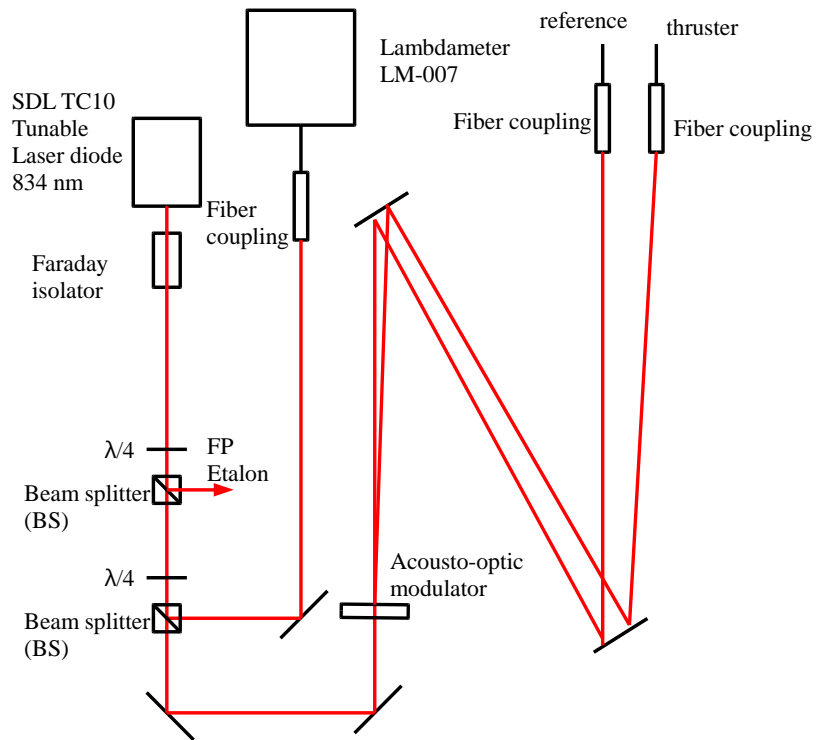| Parameter	Near field plume	Far field plume
Frequency span [GHz]	19	19 - 25
Sweep time [s]	48	170 - 190
Frequency scan speed [MHz/s]	390	130
Lock-in time constant [s]	1	3

Figure 3.   Laser optical setup

D. Wavelength calibration

A reference plasma source provides the zero-velocity reference for LIF measurements. This plasma source consists of a surface wave discharge ("surfatron") powered by microwaves at a frequency of 2.45 GHz in xenon at a typical pressure of 1 mTorr. The laser is injected in this reference discharge where a population of ions with a zero-velocity can be found. The peak of the fluorescence signal gives the reference for the frequency (and velocity) measurements.

During a frequency scan, the absolute laser wavelength is obtained by analyzing the signal of a photodiode placed behind a 230 mm confocal Fabry-Perot etalon (see an example in Figure 4). The free spectral range of the FP

is 640 MHz. By counting the transmission peaks on the photodiode signals, it is then possible to interpolate the laser frequency at each instant of the scan, and then to correct laser hysteresis. A typical LIF spectrum of the reference discharge is shown in Figure 4. The full width at half maximum of the fluorescence peak is 1300 MHz.
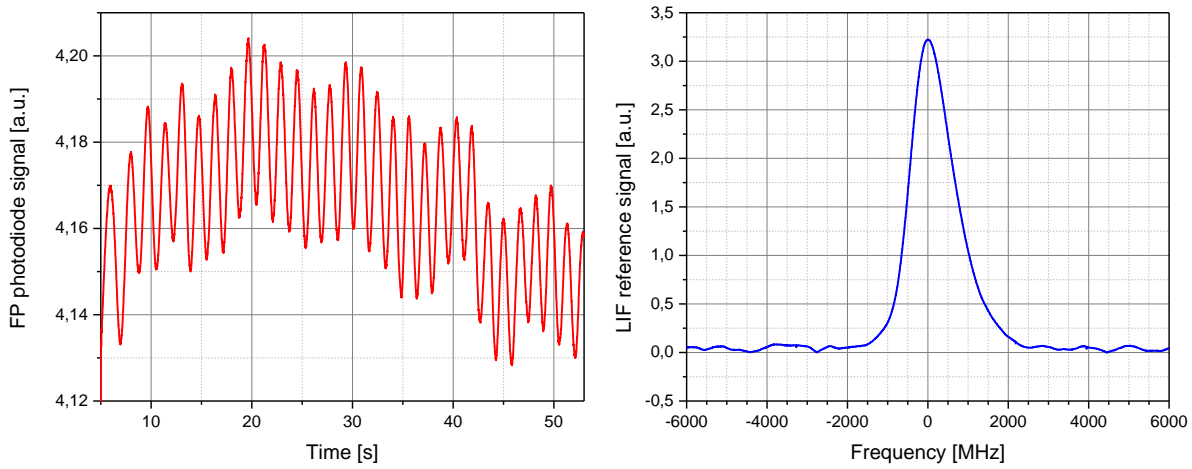

Figure 4.   Example of Fabry-Perot photodiode signal and LIF signal of the reference surfatron discharge.

E. Vacuum setup

The optics for laser injection and fluorescence detection in the vacuum chamber are shown in Figure 5. The laser is injected through a lens (25 mm diameter) and a 50 µm optic fiber. The detection is composed of a 50 mm lens and a 200 µm optic fiber. The laser axis is parallel to the thruster (magnetic nozzle) axis. The probed volume is about 1 mm diameter. The distance between the optics and the measurement point is about 450 mm, so that the perturbation of the optical setup on the plasma source is minimized. The angle between laser and detection is 35°, which ensures LIF measurements inside the thruster up to the backplate. The alignment of laser and detection optics is verified with a CCD sensor that can be placed at the measurement point. The optics are geometrically fixed in the vacuum chamber, so the probed volume cannot be moved.

The ECR thruster is placed on a 3-axis translation stage system, in order to change the longitudinal position of the measurement point along the magnetic nozzle. Moreover the LIF measurement can be performed at different azimuthal and radial positions in the source and in the plume.
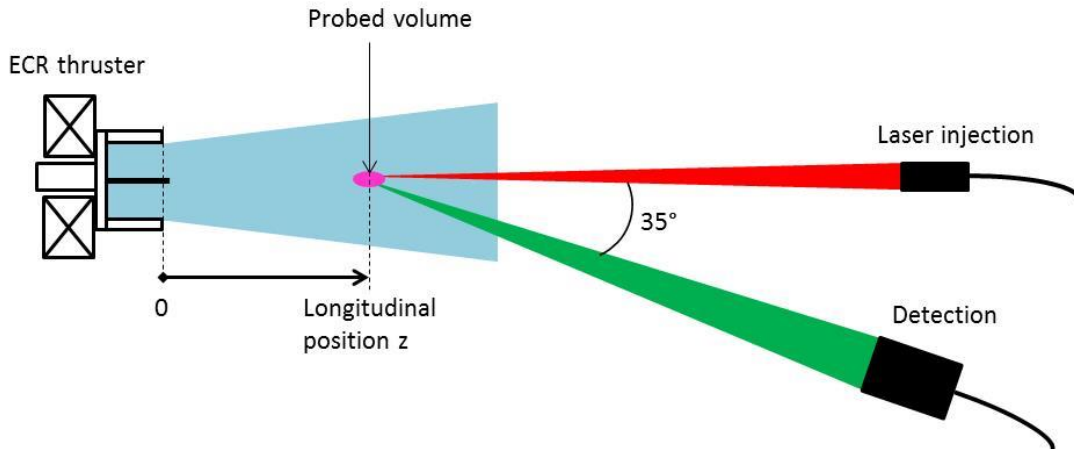

Figure 5.   Schematic of optics and thruster in the vacuum chamber

5

The experiments are led in B09 vacuum chamber at ONERA center of Palaiseau. This vacuum tank (0.8 m in diameter and 2 m long) is equipped with three Pfeiffer Hi-Pace 2300 turbo-molecular pumps that ensure a pumping speed of 2050 L/s for xenon. Recently, the pumping capacity of the system has been increased by adding a Sumitomo CH-110 cryo-cooler system. The total pumping speed of the secondary pumping system is about 13 000 L/s for xenon, with a base pressure of 10^{-7} mbar.

The ambient pressure in the vacuum chamber is measured with a Pfeiffer Compact Full Range gauge. In the conditions of the experiments (xenon flowrate between 1 and 2 sccm), the background pressure is in the range [1.2×10^{-6} - 2.5×10^{-6} mbar].

III. Results

The ECR thruster is first operated with the following conditions: xenon flowrate = 2 sccm, absorbed power = 26 W. LIF measurements are performed at different positions along the magnetic nozzle axis, from z=-5 mm (*i.e.* 5 mm inside the ECR source) to z=125 mm.

Typical examples of LIF spectra are shown in Figure 6. The LIF signals are normalized for an easier comparison of the distributions. Figure 7 shows the complete 2D mapping of the Xe$^+$ IVDF in the magnetic nozzle. Experimental data show that ion acceleration takes place over the whole measurement zone (more than 12 cm). This is to be compared to HET thrusters where the acceleration zone is about 1-2 cm.

The LIF signal is already clearly shifted inside the thruster (at z=-5 mm), and the IVDF still evolves in the far field region. It is noteworthy that broader distributions are obtained inside the thruster and close to the thruster exit. Beyond 40 mm, the distributions consist of a single narrow peak of high velocity ions. No population of slow ions is detected in the far field plume, which ensures that there is no production of secondary ions by charge exchange or electron impact in this zone. The full width at half maximum of IVDF peaks is always larger than 1.5 GHz, so the frequency resolution of the diagnostic is good enough for reliable measurements in these conditions.

The broadening of the peaks close to the thruster could be due to Zeeman splitting of the 834.7 nm transition, or to the production of slow ions. The magnetic field is higher than 200 Gauss up to 30 mm. Investigations are currently led to assess the influence of Zeeman effect on the IVDF.
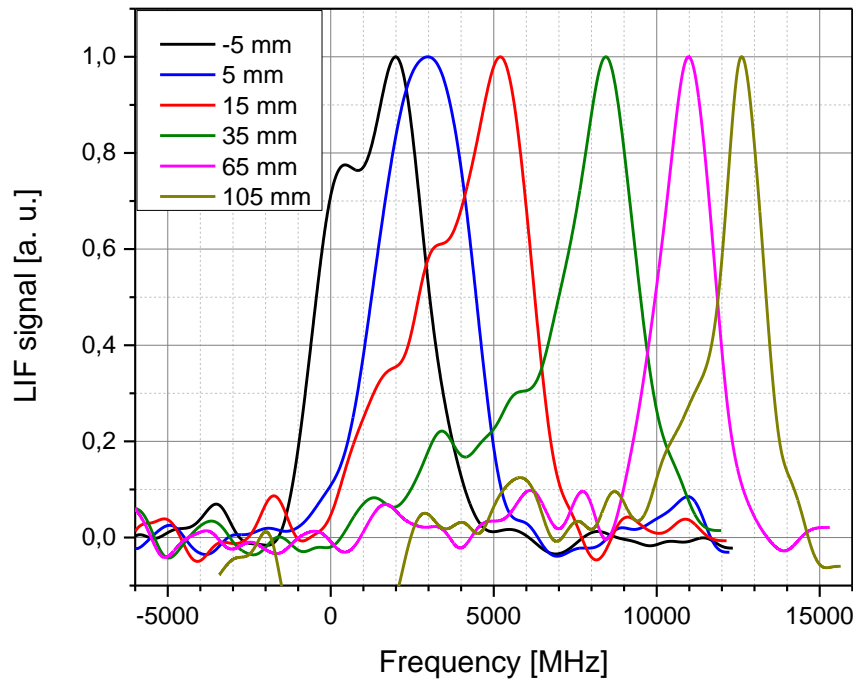

Figure 6.   Examples of LIF signals obtained at different longitudinal positions in the magnetic nozzle. Xenon flowrate: 2 sccm.
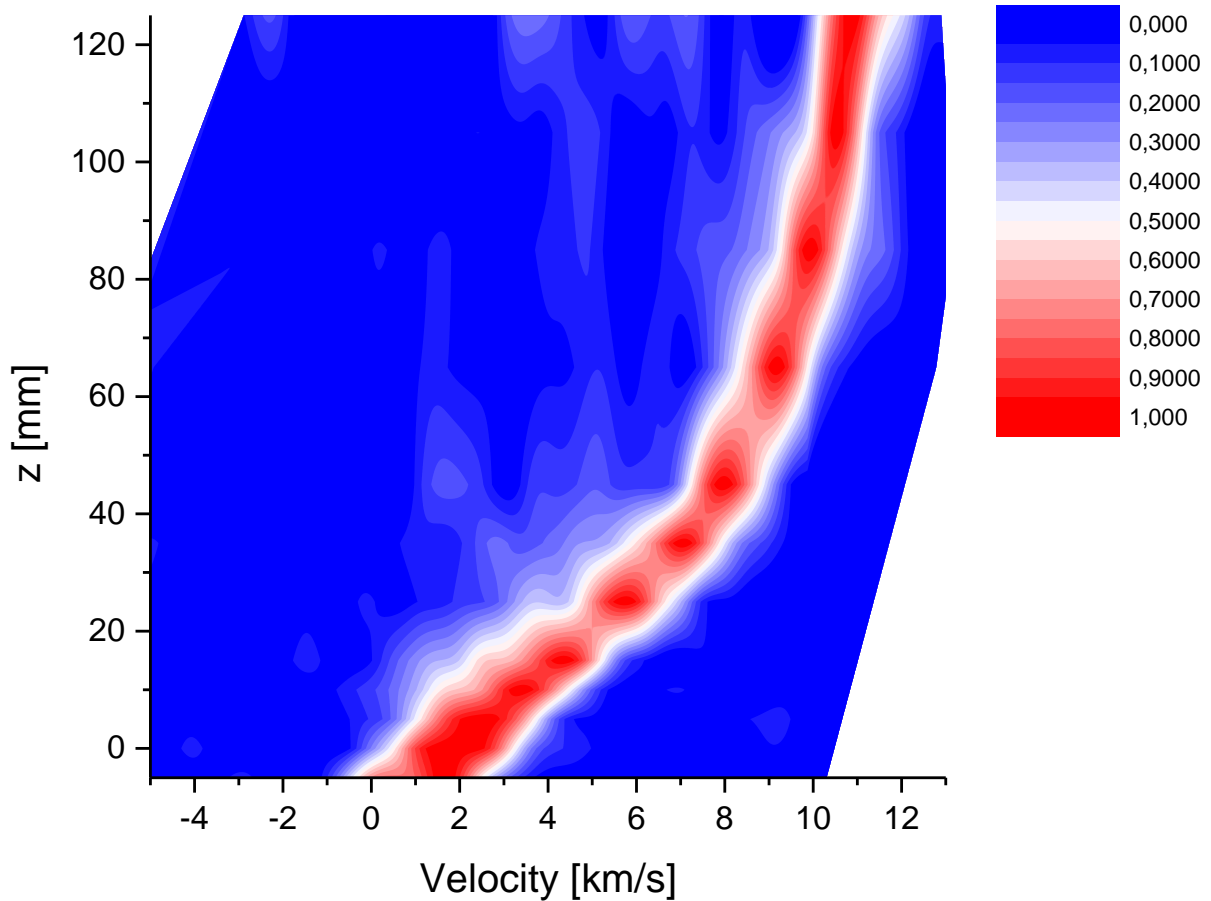
Figure 7. 2D mapping of the IVDF of Xe$^+$ in the magnetic nozzle. Xenon flowrate: 2 sccm.

LIF measurements have also been performed with two other xenon flowrates (1 and 1.5 sccm). The microwave power absorbed by the plasma is around 26 W for the three conditions. Other measurement campaigns led on ECR thruster have shown that the electron temperature in the plume [13] and in the ECR source [14] vary significantly between 1 and 2 sccm of xenon. The comparison of ion dynamics in these conditions is then interesting for the understanding of ion acceleration in the magnetic nozzle.

For every position in the magnetic nozzle, the mean axial velocity V_z of Xe$^+$ ion is determined from the IVDF. The longitudinal profiles of the mean axial velocity are compared in Figure 8 for the three operating conditions. For all positions, the highest axial velocity is obtained with the lowest mass flow rate. Due to the lower current density and the higher velocity at 1 sccm, the LIF measurements could not be performed beyond 100 mm (with the LIF parameters given in Table 1). The maximum ion velocity that could be measured for 1, 1.5 and 2 sccm is, respectively, 16.1, 12.5, and 10.9 km/s. This corresponds to an ion kinetic energy of 176, 106 and 81 eV.

However, it can be seen that the acceleration is not complete at the end of LIF measurement range. Additional measurements have been performed with a Langmuir probe (LP). The plasma potential is deduced from the inflection point of the I-V characteristics. The main drawback of LP is their intrusiveness, so the diagnostic was not placed closer than 75 mm from the thruster. Eventually LP allows to significantly extend the measurement range in the plume (up to 250 mm).

From LIF measurements, it is possible to calculate the potential drop in the plume (with respect to the maximum plasma potential in the ECR source φ_0):

$$\varphi_0 - \varphi = \frac{1}{2e}m(V_z)^2$$

7

The plasma potential (with respect to the facility ground) is then determined using the value measured with the LP in the overlapping zone of both diagnostics (between 75 and 115 mm). The electrostatic potential profiles over the whole measurement range are shown in Figure 9. The profiles are almost flat beyond 200 mm, and the value at the furthest position is taken as the asymptotic potential φ_∞. The total potential drop in the magnetic nozzle and the asymptotic value of mean axial velocity that can be estimated from LIF and LP measurements are given in Table 2. At 1 sccm, the observed potential drop is about 236 V. It can be seen that Xe$^+$ ions are accelerated up to 16 km/s in the first 100 mm of the magnetic nozzle, and they reach a value of 18.6 km/s after 250 mm.

In Figure 9 (right graph), the potential drop profile (obtained with LIF measurements) is normalized by the total potential drop: $\frac{\varphi_0 - \varphi}{\varphi_0 - \varphi_\infty}$

The relative potential drops at 105 mm are very close for the three flowrates (around 0.3). However, the profiles differ significantly, with a steeper decrease at 1 sccm. So the shape of the ambipolar electric field in the plume seems to depend on the initial conditions in the source (in particular the electron temperature in perpendicular or parallel direction).
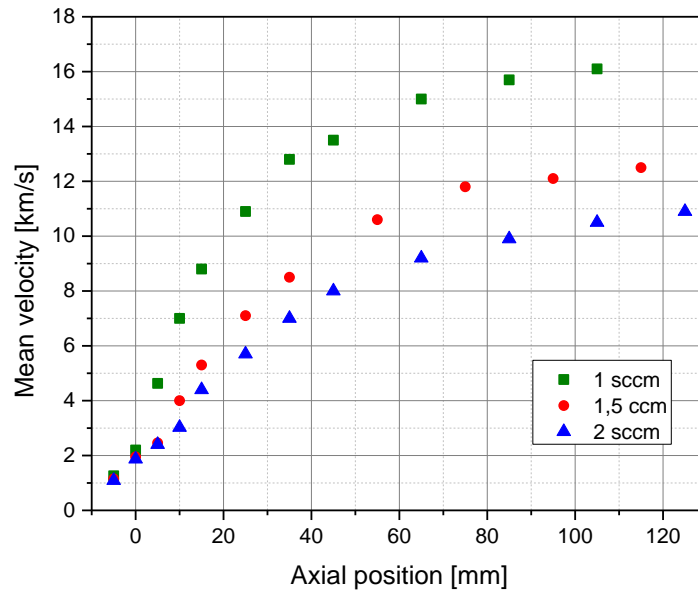

Figure 8.   Longitudinal profile of Xe$^+$ mean axial velocity in the magnetic nozzle for different xenon flow rates.
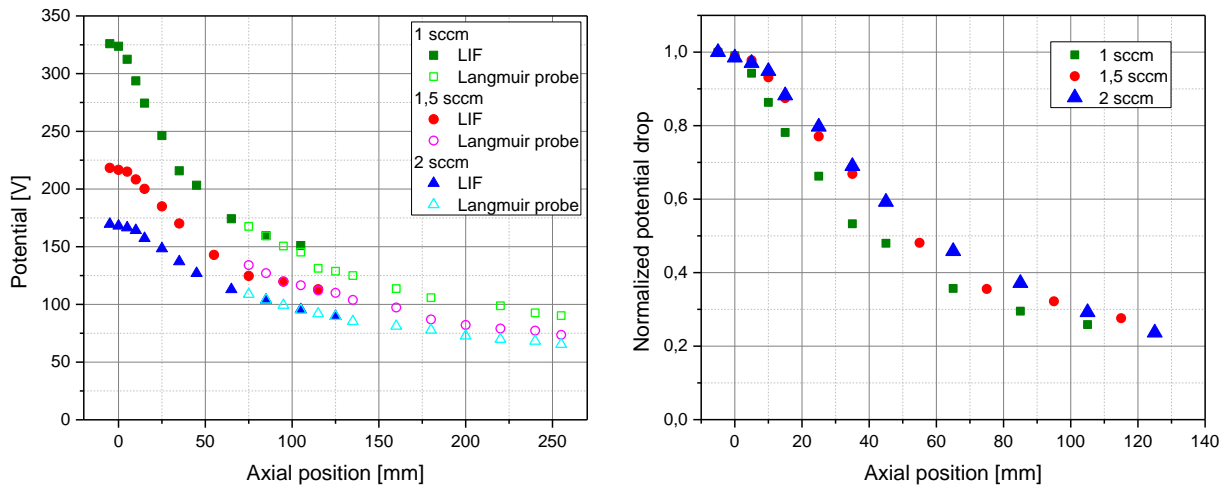

Figure 9.   Longitudinal profile of electrostatic potential along the magnetic nozzle for different xenon flowrates.

8

Table 2. Total potential drop and asymptotic axial velocity

Flowrate [sccm]	$\Phi_0\text{-}\varphi_\infty$ [V]	V_∞ [km/s]
1	236	18.6
1.5	145	14.6
2	105	12.4

IV.   Conclusion

LIF measurements have been performed in the plume of an ECR plasma thruster operated with xenon. The ion velocity distribution function allows determining the mean axial velocity of Xe^+ at different positions in the magnetic nozzle for different flowrates of xenon. The highest ion velocity (16.1 km/s) has been obtained with the lowest flowrate (1 sccm). Additional measurements with a Langmuir probe have been used to calculate the plasma potential profile in the magnetic nozzle. It has been shown that the potential is significantly affected by initial conditions in the ECR source.

Further investigations are needed to understand the influence of electron temperature on the potential profile. In particular, experimental data will be compared to a kinetic model of a magnetic nozzle. In parallel, the Zeeman effect will also be assessed to enable LIF measurements inside the source.

Acknowledgments

References

1 Jarrige, J., Elias, P.-Q., Cannat, F., and Packan, D., "Characterization of a coaxial ECR plasma thruster", Proc. 44th AIAA Plasmadynamics and Lasers Conf. (San Diego, USA, 2013).

2 Cannat, F., Lafleur, T., Jarrige, J., Chabert, P., Elias, P.-Q., and Packan, D., "Optimization of a coaxial electron cyclotron resonance plama thruter with an analytical model", Physics of Plasmas 22, 053503 (2015).

3 Vialis, T., Jarrige, J., Packan, D., "Geometry optimization and effect of gas propellant in an electron cyclotron resonance plasma thruster", Proc. 35th IEPC (Atlanta, USA, 2017), IEPC-2017-378.

4 Arefiev, A.V. and Breizman, B.N., "Ambipolar acceleration of ions in a magnetic nozzle", Physics of Plasmas, 15, 042109 (2008).

5 Ahedo, E. and Merino, M., "On plasma detachment in propulsive magnetic nozzles", Physics of Plasmas, 18, 053504 (2011).

6 Martinez-Sanchez, M., Navarro-Cavalle, J., and Ahedo, E., "Electron cooling and finite potential drop in a magnetized plasma expansion", Phys. Plasmas 22, 053501 (2015).

7 Zhang, Y., Charles, C., and Boswell, R., "Thermodynamic study on plasma expansion along a divergent magnetic field", Phys. Rev. Lett. 116, 025001 (2016).

8 Dorval, N., Bonnet, J., Marque, J., Rosencher, E., Chable, S., Rogier, F., Lasgorceix, P., "Determination of the ionization and acceleration zones in a stationary plasma thruster by optical spectroscopy study: experiments and model", J. Appl. Phys. 91, 4811-4817 (2002).

9 Mazouffre, S., Gawron, D., and Sadeghi, N., "A time-resolved laser induced fluorescence study on the ion velocity distribution function in a Hall thruster after a fast current disruption", Phys. Plasmas 16, 43504 (2009)

10 Elias, P.-Q., Packan, D., Bonnet, J., Ceccanti, F., Cesari, U., Tata, M. De Nicolini, D., Gengembre, E., "Optical Measurements of Neutral Cesium Mass Flow Rate in Field Emission Thrusters", J. Propul. Power 27, 448-460 (2011).

11 Elias, P.-Q., Jarrige, J., Cuchetti, E., Packan, D., and Bullit, A., "Full ion velocity distribution function measurement in an electric thruster, using a LIF-based tomographic reconstruction" , Proc. 34th IEPC (Kobe, Japan, 2015), IEPC-2015-235.

12 Elias, P.-Q., Jarrige, J., Cuchetti, E., Cannat, F., and Packan, D., "3D Ion velocity distribution function measurement in an electric thruster, using a LIF-based tomographic reconstruction", to be published in Rev. Sci. Instrum. (2017).

13 Lafleur, T., Cannat, F., Jarrige, J., Elias, P.-Q., and Packan, D., "Electron dynamics and ion acceleration in expanding-plasma thrusters", Plasma Sources Sci. Technol. 24, 065013 (2015).

14 Correyero, S., Jarrige, J., Packan, D., and Ahedo, E., "Measurement of anisotropic plasma properties along the magnetic nozzle expansion of an Electron Cyclotron Resonance Thruster", Proc. 35th IEPC (Atlanta, USA, 2017), IEPC-2017-437.